Geomechanics and Engineering, *Vol. 26, No. 3 (2021) 227-234*
https://doi.org/10.12989/gae.2021.26.3.227

Upper bound limit analysis of blow-out failure mode of excavation face of shield tunnel considering groundwater seepage

Fu Huang[a], Di Wang[b], Nan Xiao* and Ruo-Chen Ou[c]

School of Civil Engineering, Changsha University of Science and Technology, Changsha 410114, Hunan, China

(Received March 7, 2020, Revised July 10, 2021, Accepted August 3, 2021)

Abstract. The study of failure mode for the soil in front of a shield tunnel face is a key challenge for tunnel engineering, especially when drilling under the water table. This work aims to study face stability of a shield tunnel under the water table based on an blow-out failure mechanism in the framework of the upper bound theorem of limit analysis in conjunction with variational principle. The seepage force in the seepage field is derived, and seepage force is regarded as an external force which is introduced in the upper bound calculation. Based on the failure characteristic of the blow-out failure for the soil in front of a shield tunnel face, a upper bound failure mechanism is constructed. Using this mechanism, the equation of the failure surface is obtained and the shapes of the failure surfaces for different parameters are plotted. By studying the influence of various parameters on the shape of failure surfaces, the changing laws of the shape of the failure surface for different parameters are obtained.

Keywords: blow-out failure mechanism; Hoek-Brown failure criterion; limit analysis theorem; seepage force

1. Introduction

Shield tunnelling technology has many advantages such as safety, rapidity and a small impact on the surrounding environment and has been widely used in the construction of urban subway tunnels. Currently, the two main types of shield machines widely used in the construction of subway tunnels are the earth pressure balance shield machine and slurry shield machine. Both types of shield machines use the earth pressure (or slurry pressure) in the soil cabin (or slurry cabin) behind the cutter head to resist the water and earth pressure in front of the excavation face and maintain the stability of the excavation face. Many studies have shown that the failure modes of the soil mass are mainly divided into two categories according to the pressure of the soil cabin: collapse failure of the excavation face due to insufficient support force and blow-out failure due to excessive support force. Many researchers have studied these two failure modes. Leca and Dormieux (1990) are the scholars who first used upper -bound theorem of limit analysis to investigate these two failure modes observed in tunnel face during shield tunnel excavation. Later, Mollon *et al*. (2009) constructed a three dimensional multi-block failure mechanisms to describe the collapse and the blow-out failure modes of tunnel face in the framework of the upper-bound method in limit analysis. Using these failure mechanisms, Mollon *et al*. (2009) studied the stability of tunnel face based on a probabilistic approach. Subsequently, Mollon *et al*. (2011) proposed two rotational failure mechanisms to determine the collapse and blow-out face pressures of a circular tunnel driven by a pressurized shield. Because the proposed failure mechanisms were generated 'point by point' instead of using the existing standard geometric shapes, the upper-bound solutions of face pressures derived from these failure mechanisms are improved. Because the majority of shield tunnels are excavated in shallow stratum, most of the rock mass in the shallow stratum is heavily fractured. Thus, to investigate the face stability of tunnels excavated in fractured and cracked rock masses, Senent *et al*. (2013) developed an advanced rotational failure mechanism. Using this failure mechanism, Senent *et al*. (2013) computed the collapse pressure for tunnel faces in conjunction with the Hoek-Brown non-linear failure criterion. In a further study, Mollon *et al*. (2013) proposed new failure mechanisms to investigate the face stability of shield tunnels excavated in purely cohesive soils. By comparing their mechanisms with existing results, Mollon *et al*. (2013) pointed out that the collapse pressures calculated by their approach are better than the best existing solutions. Based on the rotational failure mechanism proposed by Mollon *et al*. (2011), Ibrahim *et al*. (2015) developed an improved failure mechanism to study the face stability of tunnels excavated in dry multilayered purely frictional soil. More recently, some scholars (Zhang *et al.* 2018, Li and Yang 2019, Zhang *et al.* 2020) also investigated the failure modes of shield tunnel face in the framework of the limit analysis theorem.

When a shield tunnel passes through water-rich strata, groundwater seepage has a great influence on the stability

*Corresponding author, Ph.D., Lecturer
E-mail: xn@csust.edu.cn
[a]Ph.D., Associate Professor
E-mail: hfcsu0001@163.com
[b]Master Student
E-mail: wd874855411@163.com
[c]Master Student
E-mail: arlo_ou@126.com

ISSN: 2005-307X (Print), 2092-6219 (Online)

of the shield tunnel face. News media have reported many stability accidents in tunnel faces due to groundwater seepage, resulting in relatively serious economic losses and casualties. In view of the adverse effects of groundwater on the stability of the tunnel face, some scholars have begun to study this issue. Based on the limit equilibrium method, Perazzelli *et al*. (2014) derived a closed-form solution for the necessary face support pressure of a tunnel excavated under seepage flow conditions. To study the influence of pore water pressure on tunnel face stability, Pan and Dias (2016) calculated the supporting pressure of a circular tunnel driven below the water table on the basis of the upper bound theorem of limit analysis. Subsequently, Pan and Dias (2018) investigated the face stability of a circular tunnel in weak rock masses under the water table. Combining the limit analysis method with the strength reduction technique, Li *et al*. (2019) calculated the safety factor of a tunnel excavated under steady unsaturated seepage conditions. Moreover, by comparing their results with previous studies, the validity of the approach proposed by Li *et al*. (2019) is proved. To obtain the support pressure required to keep the stability of tunnel face under a seepage flow condition, Sahoo and Kumar (2019) established a model on the basis of the finite element limit analysis in conjunction with the limit analysis theorem. Using this model, Sahoo and Kumar (2019) calculated the required support pressures of tunnel face for different positions of groundwater table above tunnel crown. Furthermore, some scholars also used their model test to study this issue. Lv *et al*. (2018) developed a centrifuge model test device to investigate the failure mechanism and limit support pressure of a shield tunnel face under a seepage condition. By using a particle image velocimetry technique, they obtained the failure mechanism of the tunnel face which is reflected by soil particle movements. More recently, Chen *et al*. (2018) employed a centrifuge model test to study the collapse mode of the tunnel face induced by the steady state seepage in the saturated sandy silt. Based on the experimental data, they found that the difference of hydraulic head between the ground and the chamber significantly affects the limit effective support pressure.

While some scholars have studied the failure modes of shield tunnel excavation faces under the condition of groundwater seepage, most such studies have been carried out on the collapse failure of the excavation face caused by an insufficient setting of the soil tank pressure of the shield machine. However, few scholars have studied the phenomenon of soil blow-out failure in front of the excavation face caused by an excessively high soil tank pressure setting underground water seepage conditions. This paper constructs a kinematically admissible velocity field suitable for this condition based on the blow-out failure characteristics of the soil mass in front of the excavation face caused by an excessively high earth pressure setting of the shield machine underground water seepage. The external force power and the internal dissipation rate of energy in the failure mechanism are calculated by the equation of virtual work, and an objective function containing the equation of the blow-out failure curve is obtained. On this basis, and using the variational principle, an analytical expression of soil blow-out failure in front of the excavation face of a shield tunnel under the limit state is calculated. The shape of the soil blow-out failure surface and the scope of damage in front of the excavation face are derived according to the equation. The research results in this paper can provide a theoretical basis for the study of the blow-out failure mode of a soil mass in front of a tunnel face in water-rich strata.

2. Upper limit calculation of blow-out failure mode for shield tunnel face considering groundwater seepage

2.1 Blow-out failure mechanism of shield tunnel excavation face considering groundwater seepage

In the excavation process of a shield machine, if the pressure value in the soil tank is set too high, the soil in a certain range in front of the cutter head will have minor displacement in front of the excavation face at a certain rate under the action of the soil tank pressure. When the displacement is transmitted in the soil and finally reaches the ground surface, the soil within the affected area will undergo blow-out type failure. Based on the mechanism of the blow-out failure of soil mass in front ofa shield tunnel excavation face and the results of Huang *et al*. (2018), the blow-out failure mechanism of a shield tunnel excavation face considering groundwater seepage is established (Fig. 1).The failure mechanism consists of an arbitrary curve z(y) extending from point O at the bottom of the excavation face to point R of the ground surface and a straight line extending from point P at the top of the tunnel to point Q on the ground surface. The soil mass in front of the tunnel excavation face is pushed by the pressure of the soil tank, and the soil will move slightly along the curve and the straight line, causing the velocity on the curve to be discontinuous. Therefore, the failure surface can also be called the velocity discontinuity surface. In addition, the rock/soil mass between curve OR and line PQ is the compressively damaged mass formed by the earth pressure on the soil in front. Since the curve constituting the failure mechanism does not need to be preset to a line shape, the artificial intervention can be excluded to the greatest extent in the calculation process, thereby allowing the rock and soil failure shape closest to the actual situation to be achieved.

It is assumed that the soil within a certain range in front of the excavation face forms a rigid damaged mass under the compression of the soil tank pressure. Under the action of the compressing force, the damaged body has relative motion with velocity v at an angle β with the horizontal direction, and the damaged mass velocity vector and the coordinate system direction are as shown in Fig. 1.The diameter of the shield tunnel is D, the distance from the top of the tunnel to the ground surface is L, and the distance from the groundwater head to the top of the shield tunnel is H (assuming the water head is higher than the ground line). It is assumed that the soil tank pressure of the shield machine is σ_T, which is evenly distributed over the entire excavation face.

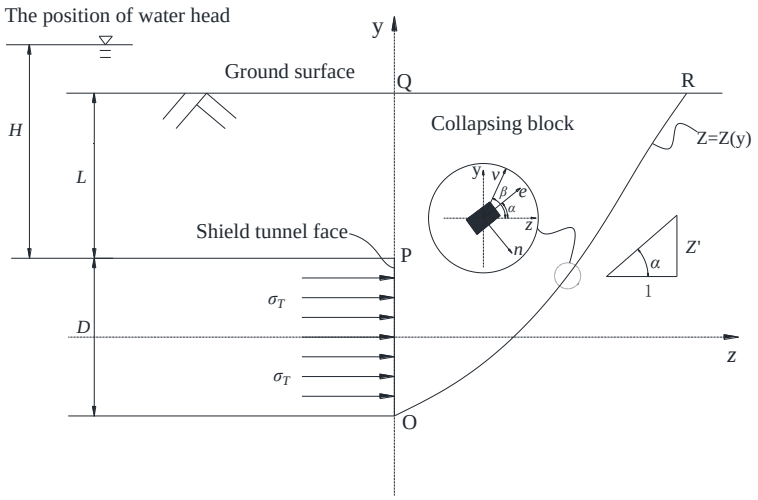

Fig. 1 Mechanism of soil blow-out failure in front of excavation face underground water seepage

2.2 Seepage field analysis

This paper considers the influence of groundwater seepage on the blow-out failure mode of a shield tunnel. Therefore, it is necessary to analyze the seepage field in front of the excavation face during tunneling. According to the upper bound limit analysis, the objective function for solving the curve containing the failure surface comprises the internal dissipation rate of energy and the external force power in the failure mechanism. The external forces in the upper bound failure mechanism of the shield tunnel under the groundwater seepage flow constructed in this paper include the damaged body weight, the soil tank pressure and the seepage force. Therefore, we first must calculate the seepage force in the seepage field. In the two-dimensional seepage field, the drag force (f_x, f_y, f_z) of the seepage water on the soil particles per unit area of soil is represented by the following formula:

$$f_z = -\gamma_\omega \frac{\partial h}{\partial z}, f_y = -\gamma_\omega \frac{\partial h}{\partial y} \tag{1}$$

where h is the total water head, and γ_ω is the unit weight of water. The Gauss integral theory is applied to the unit area seepage force of the sliding body in front of the excavation face, and the horizontal and vertical component expressions of the seepage force acting on the sliding body are obtained:

$$F_z(\beta) = \gamma_\omega(-\sin\beta\int_{S1} h^* ds + \int_{S2} h^* ds) \tag{2}$$

$$F_y(\beta) = \gamma_\omega(\cos\beta\int_{S1} h^* ds + \int_{S2} h^* ds) \tag{3}$$

where S1 is the damaged mass velocity discontinuity surface, S2 is the tunnel excavation face, and h^* is the average water head in the horizontal direction inside the damaged mass, which can be calculated by the following equation:

$$h^* = \frac{1}{D}\int h(z,y)dy \tag{4}$$

The seepage force components in the seepage field can be expressed as

$$\begin{aligned} F_z(\beta) &= \gamma_\omega\left(-\sin\beta\int_{S1} h^* ds + \int_{S2} h^* ds\right) \\ &= \gamma_\omega\int_{-y_0}^{y_0}\left[-\sin\beta\left(H+\frac{D}{2}\right)\sqrt{1+z'^2} + (H+\frac{D}{2})\right]dy \end{aligned} \tag{5}$$

$$\begin{aligned} F_y(\beta) &= \gamma_\omega\left(\cos\beta\int_{S1} h^* ds - \int_{S2} h^* ds\right) \\ &= \gamma_\omega\int_{-y_0}^{y_0}\left[\cos\beta\left(H+\frac{D}{2}\right)\sqrt{1+z'^2} + (H+\frac{D}{2})\right]dy \end{aligned} \tag{6}$$

where D is the shield tunnel diameter, β is the angle between the damaged body and the horizontal direction, and H is the distance between the groundwater head and the top of shield tunnel.

2.3 Energy consumption calculation of soil blow-out failure in front of excavation face of shield tunnel based on Hoek-Brown failure criterion

In the process of calculating the soil failure surface in front of a tunnel excavation face via the upper bound limit analysis, it is necessary to calculate the internal dissipation rate of energy generated on the failure surface. According to the theory proposed by Chen (1975), the internal dissipation rate of energy at any point in the plastic flow region can be obtained from the plastic stress/strain relationship. Therefore, we first must find a yield function to describe the stress/strain relationship of the rock/soil mass under plastic flow conditions. The Hoek-Brown nonlinear failure criterion can reflect the nonlinear failure characteristics of rock/soil mass and can effectively evaluate the strength of loose and fractured rock/soil mass (Huang *et al.*2020). In this paper, the Hoek-Brown failure criterion (H-B failure criterion) expressed in the form of principal stress and shear stress is used to calculate the stress and strain of rock/soil mass in the plastic flow zone. The failure criterion can be expressed by the following formula:

$$\tau = A\sigma_c\left(\frac{\sigma_n - \sigma_t}{\sigma_c}\right)^B \tag{7}$$

where A and B are the dimensionless parameters of rock/soil mass; τ and σ_n are the shear stress and principal stress, respectively; σ_c is the uniaxial compressive strength of rock/soil mass; and σ_{tm} is the tensile strength of rock/soil mass. To simplify the calculation process, let $A\left(\frac{1}{\sigma_c}\right)^{B-1} = E$; the above equation then can be simplified to

$$\tau = E(\sigma_n - \sigma_t)^B \tag{8}$$

If the rock/soil mass is assumed to obey the associated flow law, then the plastic potential surface coincides with the yield surface when the rock/soil mass fails; the plastic potential function can be expressed by the yield function:

$$G = \tau - E(\sigma_n - \sigma_t)^B \tag{9}$$

When the rock/soil mass undergoes plastic failure, it is assumed that the rock/soil mass obeys the associated flow rule, and the increase in strain at this time is proportional to the stress gradient of the potential function:

$$\begin{cases} (\dot{\varepsilon}_n)_i = \lambda\dfrac{\partial G}{\partial \sigma_n} = -\lambda EB\left(\sigma_n - \sigma_t\right)^{B-1} \\ (\dot{\gamma}_n)_i = \dfrac{\partial G}{\partial \tau} = \lambda \end{cases} \tag{10}$$

where λ is the plastic multiplier. The failure mechanism of soil blow-out failure in front of the tunnel excavation face is assumed to be an arbitrary curve $z(y)$. Assuming that α_i is the angle between the tangent vector of any point on $z=z(y)$ and the z-axis, the tangent of the angle between any point on the failure curve and the z-axis can be represented by the first derivative of the failure surface curve; i.e., $\tan\alpha_i = z'(y)$. According to the geometric relationship shown in Fig. 1, the increase in normal strain and tangential strain on the velocity discontinuity surface can be obtained, where d is the assumed plastic flow zone thickness:

$$\begin{cases} (\dot{\varepsilon}_n)_i = -\dfrac{v\sin(\beta - \alpha_i)}{d} \\ (\dot{\gamma}_n)_i = \dfrac{v\cos(\beta - \alpha_i)}{d} \end{cases} \tag{11}$$

The following relation can be obtained by combining the above formulas:

$$\lambda = \frac{v}{d}\cos(\beta - \alpha_i) \tag{12}$$

$$\begin{cases} \tau_n = E\left[EB\cot\left(\beta - \alpha_i\right)^{\frac{B}{1-B}}\right]^{\frac{B}{1-B}} \\ \sigma_n = \sigma_t + \left[EB\cot\left(\beta - \alpha_i\right)\right]^{\frac{1}{1-B}} \end{cases} \tag{13}$$

The internal dissipation rate of energy $\Delta\dot{D}_i = \sigma_i\dot{\varepsilon}_i$ at any point on the failure curve $z=z(y)$ is

$$\begin{aligned} \Delta\dot{D}_i &= \sigma_i\dot{\varepsilon}_i + \tau_i\dot{\gamma}_i \\ &= \frac{v\sin(\beta - \alpha_i)}{d}\left\{-\sigma_t + \cot\left(\beta - \alpha_i\right)^{\frac{1}{1-B}}\left[-(EB)^{\frac{1}{1-B}} + E(EB)^{\frac{B}{1-B}}\right]\right\} \end{aligned} \tag{14}$$

where

$$\sin\left(\beta - \alpha\right) = \frac{\sin\beta - z'\cos\beta}{\sqrt{1+z'^2}}, \cot\left(\beta - \alpha\right) = \frac{1 + z'\tan\beta}{\tan\beta - z'} \tag{15}$$

To simplify calculation process, let

$$\bar{E} = -(EB)^{\frac{1}{1-B}} + E(EB)^{\frac{B}{1-B}} \tag{16}$$

The internal dissipation rate of energy is integrated over the entire failure surface, and considering the internal dissipation rate of energy in the linear failure mechanism, the total internal dissipation rate of energy on the failure surface is

$$\begin{aligned} W_D &= \int_{-\frac{D}{2}}^{\frac{D}{2}+L}\left(\Delta D + cL\sin\beta\right)\mathrm{d}s \\ &= \int_{-\frac{D}{2}}^{\frac{D}{2}+L}\left\{\left(\sin\beta - z'\cos\beta\right)\left[-\sigma_t + \bar{E}\left(\frac{1+z'\tan\beta}{\tan\beta - z'}\right)^{\frac{1}{1-B}}\right] + \frac{cL\sin\beta}{D+L}\right\}v\mathrm{d}y \end{aligned} \tag{17}$$

where c is the cohesive force of rock mass. The power of gravity on the failure surface is

$$\dot{W}_G = -\int_{-\frac{D}{2}}^{\frac{D}{2}+L}\gamma z v\sin\beta\mathrm{d}y \tag{18}$$

where γ is the unit weight of rock/soil mass (unit: kN/m^3). The power generated by the soil tank pressure during the tunneling of the shield machine is

$$\dot{W}_C = D\sigma_T\cos\beta v \tag{19}$$

where σ_T is the soil tank pressure of the shield machine. Using the seepage force formulas shown in Eqs. (5) and (6), the seepage power acting in the upper bound limit failure mechanism can be calculated by the following formula:

$$\dot{W}_\omega = -\int_{-\frac{D}{2}}^{\frac{D}{2}+L}\gamma_\omega\left(H + \frac{D}{2}\right)\left(\sin\beta - \cos\beta\right)\mathrm{d}y \tag{20}$$

The upper bound theorem of limit analysis shows that the external force power and the internal dissipation rate of energy in the failure mechanism satisfy the following relationship:

$$\dot{W}_G + \dot{W}_C + \dot{W}_\omega \le W_D \tag{21}$$

To obtain the failure surface analytical equation, an objective function containing the failure surface equation must be constructed according to the external force power and the internal dissipation rate of energy.

$$\begin{aligned} J &= W_D - \left(W_G + W_C + W_\omega \right) \\ &= \int_{-\frac{D}{2}}^{\frac{D}{2}+L} \left\{ (\sin\beta - z'\cos\beta) \left[-\sigma_t + \bar{E} \left(\frac{1+z'\tan\beta}{\tan\beta - z'} \right)^{\frac{1}{1-B}} \right] + \gamma_\omega \left(H + \frac{D}{2} \right) (\sin\beta - \cos\beta) \right. \\ &\quad \left. + \gamma z \sin\beta - \frac{\sigma_T \cos\beta}{D+L} + \frac{cL\sin\beta}{D+L} \right\} v \mathrm{d}y \\ &= \int_{-\frac{D}{2}}^{\frac{D}{2}+L} F[y, z(y), z'(y)] v \mathrm{d}y \end{aligned} \tag{22}$$

where

$$\begin{aligned} F(y,z,z') &= (\sin\beta - z'\cos\beta) \left[-\sigma_t + \bar{E} \left(\frac{1+z'\tan\beta}{\tan\beta - z'} \right)^{\frac{1}{1-B}} \right] + \gamma_\omega \left(H + \frac{D}{2} \right) (\sin\beta - \cos\beta) \\ &\quad + \gamma z \sin\beta - \frac{\sigma_T \cos\beta}{D+L} + \frac{cL\sin\beta}{D+L} \end{aligned} \tag{23}$$

According to the upper bound limit theorem, the corresponding failure curve equation $z(y)$ is the true upper bound solution only when the objective function J takes the extreme value. As seen in Eq. (22), the objective function J is completely determined by the function $F(y,z,z')$. Therefore, the equation of the soil failure surface in front of the tunnel excavation face in the limit state sought in this paper is to solve for the failure curve $z(y)$ equation corresponding to $F(y,z,z')$ as the limit value. In addition, the independent variables of $F(y,z,z')$ already contain z and z'. Therefore, $F(y,z,z')$ is a functional. Since F does not contain y-i.e., $F=F(y,z,z')$-at this point, the extremum of the solution of $F(z,z')$ is solved by solving the solution of its corresponding Euler equation under fixed boundary conditions. Integrating Eq. (23) can obtain

$$F - z' \frac{\partial F}{\partial z'} = c_1 \tag{24}$$

Substituting Eq. (23) into Eq. (24) can obtain

$$\frac{\partial F}{\partial z'} = \sigma_t \cos\beta - \bar{E}\cos\beta \left(\frac{1+z'\tan\beta}{\tan\beta - z'} \right)^{\frac{1}{1-B}} + \frac{\bar{E}}{(1-B)\cos\beta} \frac{(1+z'\tan\beta)^{\frac{B}{1-B}}}{(\tan\beta - z')^{\frac{1}{1-B}}} \tag{25}$$

Simplification of the above equation obtains

$$\begin{aligned} &\bar{E} \left(\frac{1+z'\tan\beta}{\tan\beta - z'} \right)^{\frac{1}{1-B}} \left[\sin\beta - \frac{z'}{(1-B)(1+z'\tan\beta)\cos\beta} \right] - \sigma_t \sin\beta + \gamma z \sin\beta \\ &- \frac{\sigma_T \cos\beta}{D+L} + \frac{cL\sin\beta}{D+L} + \gamma_\omega \left(H + \frac{D}{2} \right) (\sin\beta - \cos\beta) = c_1 \end{aligned} \tag{26}$$

This can solve for $z'=\varphi(z,c_1)$, and the group of limit value curves can be obtained after integration:

$$y = \int \frac{\mathrm{d}z}{\varphi(z, c_1)} + c_2 \tag{27}$$

where c_1 and c_2 are the integration constants to be determined. Analysis of Equation (26) shows that the selection of the parameter B is extremely important for solving the objective equation. In the Hoek-Brown nonlinear failure criterion, B is a material parameter and ranges from 0 to 1. It can be found from the observation that when B=0.5, the index of Eq. (26) is 2, and the solution of Euler's equation can be obtained by numerical analysis software. When B takes a value other than 0.5, Eq. (26) is a complicated nonlinear differential equation, and the solution of the equation cannot be obtained. Therefore, this paper discusses the analytical solution of the failure surface equation of the soil mass in front of the excavation face of a shield tunnel only when B=0.5. When B=0.5, the obtained equation of the soil blow-out failure surface in front of the excavation face is

$$\begin{aligned} y = c_2 - \Big\{ & 2\cos\beta \Big\{ \Big\{ \bar{E}^2 \cos^2\beta - \bar{E}\sin\beta [c_1 + \sigma_t \sin\beta + \sigma_T \cos\beta \\ & + \gamma_\omega \left(\frac{D}{2} + H \right) (\cos\beta - \sin\beta) - L\sigma_c \sin\beta / (D+L)] \\ & + \bar{E}\gamma z (1 - \cos^2\beta) \Big\} \Big/ \cos^2\beta \Big\}^{\frac{1}{2}} - \gamma z \cos\beta + \gamma z \cos^3\beta \Big\} \\ & / \left(\gamma \sin\beta - \gamma \cos^2\beta \sin\beta \right) \end{aligned} \tag{28}$$

According to the upper bound failure mechanism shown in Fig. 1, the failure surface curve satisfies the geometric condition $y(0) = -\frac{D}{2}$. In addition, since the excavation face of the shield machine is a free surface, there is no shear stress at this place, so the shear stress at the junction of the tunnel excavation face and the failure surface is zero:

$$\tau_{zy} \left(y = -\frac{D}{2} \right) = 0 \tag{29}$$

Taking a microelement at the junction of the tunnel excavation face and the failure surface to establish a stress balance equation can result in

$$\tau_{zy} = \tau_n \cos^2\theta - \tau_n \sin^2\theta - \sigma_n \sin\theta\cos\theta \tag{30}$$

Eq. (30) is transformed by a trigonometric function to obtain the following relationship:

$$2\tau_n \cos 2\theta = \sigma_n \sin 2\theta \tag{31}$$

According to the triangular relationship between the shear stress and the angle between the y-axis at any point on the surface of the failure surface shown in Fig. 1, the following can be obtained:

$$\sin\theta = \frac{y'}{\sqrt{1+y'^2}}, \cos\theta = \frac{1}{\sqrt{1+y'^2}} \tag{32}$$

By substituting Eqs. (32) and (13) into Equation (31), the integral constant c_1 can be obtained. The geometrical boundary condition (29) is used to find integral constant c_2, and then integral constants c_1 and c_2 are substituted into Equation (28).The analytical equation of the failure surface of the soil mass in front of the tunnel face of the shield tunnel then can be obtained.

3. Analysis of calculation results

3.1 Comparison with numerical simulation results

To evaluate the validity of the formula for failure surface derived in this paper, the analytical solution was compared with the results derived from the numerical

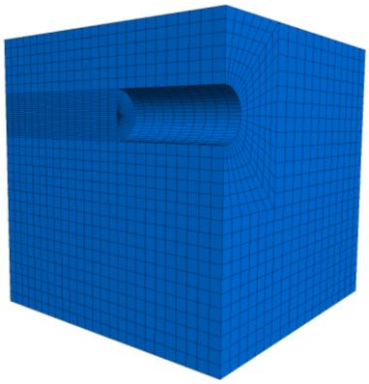

Fig. 2 Numerical model for the stability analysis of the shield tunnel face

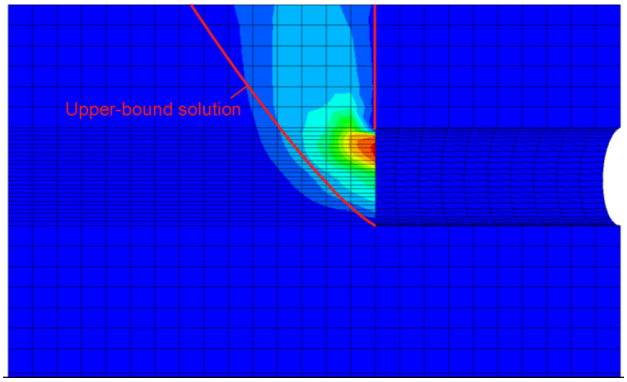

Fig. 3 Comparison of the failure surface provided by the upper-bound theorem and the numerical simulation

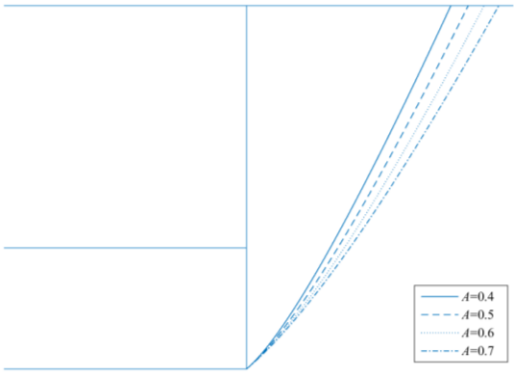

Fig. 4 Blow-out failure shape of tunnel excavation face under different values of A

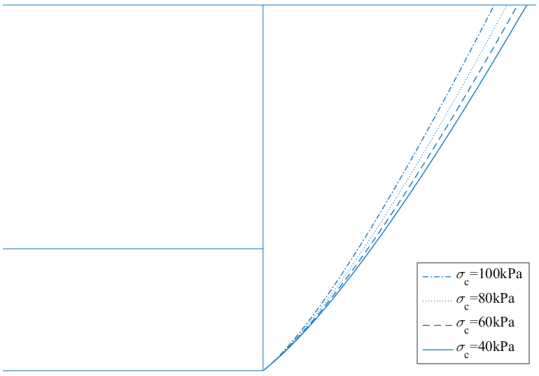

Fig. 5 Blow-out failure shape of tunnel excavation face under different values of σ_c

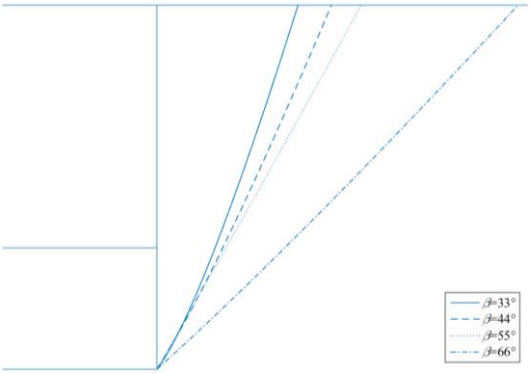

Fig. 6 Blow-out failure shape of tunnel excavation face under different values of β

simulation software FLAC3D. A 3D numerical model was constructed to simulate the failure characteristic of the blow-out failure for the soil in front of a shield tunnel face. The diameter of the shield tunnel is 8 m, and the depth from the tunnel roof to the ground surface is 10 m. The dimensions of the numerical model are all taken as 50 m in the transversal, longitudinal, and vertical directions, which can be seen in Fig.2. To simulate the seepage field below the water table, the mechanical boundary conditions and hydraulic boundary conditions must be set. The mechanical boundary conditions are assumed as follows: the vertical displacements at the undersurface of the model are fixed, and only the horizontal directions are fixed on the vertical boundaries. For the hydraulic boundary conditions, the pore-water pressure in the soil cabin is assumed to be zero, and the groundwater table measured from the tunnel roof is equal to the water head H which is assumed to stay constant for the steady-state fluid flow analysis.

Moreover, the H-B criterion represented by normal and shear stresses is used in the upper-bound calculation and the H-B criterion represented in terms of the major and minor principal stresses are employed in the numerical simulation. Because the parameters of the two forms of the H-B criterion are different, it is necessary to convert the parameters in one form of the H-B failure criterion into the parameters in another form equivalently. Based on the method presented by Huang *et al*. (2018), the parameters used in the two forms of the H-B criterion are converted equivalently and a comparison between the upper-bound calculation and the numerical simulation under the same condition can be conducted. Using the equivalent parameters and the simulation model, the contours of the displacement for the tunnel face that reflect the shape failure surface were obtained, which can be seen in Fig. 3. Furthermore, the upper bound solution of failure surface obtained from Equation (28) is superimposed in Fig. 3. It can be seen from Fig. 3 that the upper-bound solution of the failure surface is approximately in accordance with the failure surface provided by numerical simulation. The good agreement between the two methods for the tunnel failure surface indicates that the theoretical formulas derived in this paper are valid.

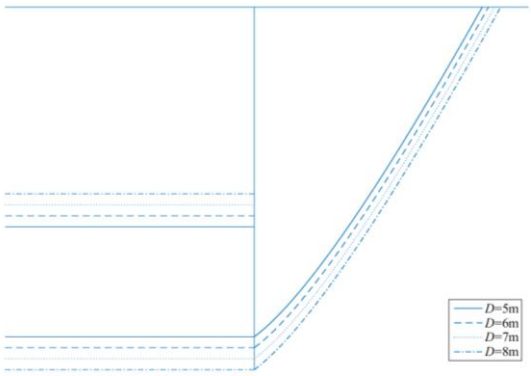

Fig. 7 Blow-out failure shape of tunnel excavation face under different values of D

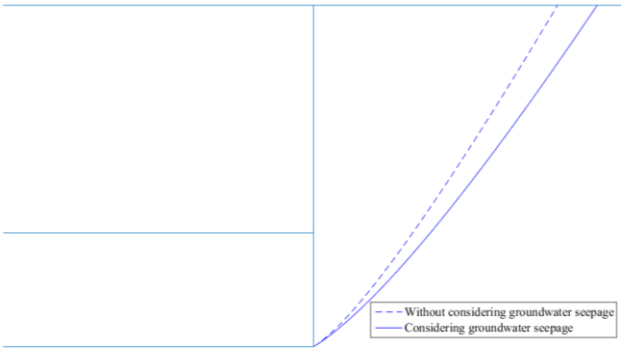

Fig. 8 Effect of groundwater seepage on blow-out failure shape of tunnel excavation face

3.2 Parametric analysis

Based on the blow-out failure surface equation of the soil mass in front of the excavation face of a shield tunnel obtained from the upper bound calculation, the shape of the blow-out failure surface under the limit state can be drawn using software. To study the influence of different parameters on the shape and extent of soil failure in front of the tunnel face, the shapes of the failure surfaces of the soil mass in front of the tunnel excavation face were drawn using the parameters of β=33-66°, B=0.5, A=0.4-0.7, σ_c=40-100 kPa, σ_t=0, D=5-8 m, L=10 m, H=10 m, c=10 kPa, σ_T=800kN, and γ=7.5kN/m^3; the results are shown in Figs. 4 to 7.

The figures show that the blow-out failure of the soil mass in front of the excavation face occurred under the action of excessive soil tank pressure. The failure surface curve extends from the bottom of the excavation face to the ground surface and intersects the ground line. The soil within the curve tends to bulge toward the surface. The soil mass in the range between intersection point R of the surface of the earth with the curve and point Q directly above the excavation face can be considered as the blow-out failure area of the soil mass in front of the excavation face when the pressure of the soil tank of the shield machine is too high. In addition, different parameters have a great influence on the extent of soil failure in front of the tunnel face. When other parameters are constant, the extent of soil failure in front of the excavation face increases with increasing A, β and D. In contrast, when the other parameters are constant, the extent of soil failure in front of the excavation face decreases as σ_c increases.

Table 1 Length of extent of soil failure l in front of excavation face under different parameters

Number	A	B	σ_c(kPa)	β(°)	D(m)	H(m)	γ(kN/m^3)	l (m)
1	0.4	0.5	70	33	5	10	7.5	16.78
2	0.5	0.5	70	33	5	10	7.5	18.33
3	0.6	0.5	70	33	5	10	7.5	19.65
4	0.7	0.5	70	33	5	10	7.5	20.85
5	0.5	0.5	40	33	5	10	7.5	20.12
6	0.5	0.5	60	33	5	10	7.5	19.17
7	0.5	0.5	80	33	5	10	7.5	18.05
8	0.5	0.5	100	33	5	10	7.5	17.16
9	0.5	0.5	70	44	5	10	7.5	22.62
10	0.5	0.5	70	55	5	10	7.5	26.51
11	0.5	0.5	70	66	5	10	7.5	47.01
12	0.5	0.5	70	33	6	10	7.5	18.89
13	0.5	0.5	70	33	7	10	7.5	19.33
14	0.5	0.5	70	33	8	10	7.5	19.94

To analyze the influence of the groundwater seepage effect on the extent of soil mass failure in front of the tunnel face, the damage extent of the soil mass in front of the tunnel face with and without the consideration of groundwater seepage was drawn. A comparison of the scope of the failure in these two cases is shown in Fig. 8.When the other parameters remain unchanged, the extent of the soil failure in front of the excavation face of the shield tunnel increases obviously when considering the groundwater seepage (Fig. 8).Therefore, when the shield machine is driven in a groundwater-rich formation, the influence of the groundwater seepage effect on the extent of soil failure in front of the tunnel face must be considered.

In addition, to quantify the extent of soil failure in front of the excavation face, this paper assumes that the distance l from intersection point R of the failure surface curve to point Q directly above the excavation face is the length of the extent of soil failure in front of the excavation face. This value is used as the basis for measuring the range of the failure. According to the failure surface equation of the soil mass in front of the tunnel excavation face, the length l of the extent of soil failure in front of the excavation face under different parameters is calculated, as shown in Table 1. Using Table 1, the specific values of the length of the soil failure in front of the shield excavation face can be directly determined according to the surrounding rock parameters and the tunnel size, thus providing a theoretical basis for the treatment of surface bulging.

4. Conclusions

This paper presents an upper bound failure mechanism for the blow-out failure characteristics of the soil mass in front of the excavation face of a shield tunnel caused by excessively high soil tank pressure of the shield machine.

Groundwater seepage is considered. On this basis, the analytical solution of the soil failure surface equation is derived via upper bound limit analysis and variational theory. According to the analytical equation of the failure surface, the failure shape and failure extent of the soil blow-out failure surface in front of the excavation face are drawn, and the influence of a single parameter change on the extent of soil failure is analyzed. The analysis results show that the parameters A, β, σ_c and D affect the extent of the soil failure in front of the excavation face when considering groundwater seepage. When the other parameters are constant, the extent of soil failure in front of the excavation face increases as A, β and D increase and decreases as σ_c increases. Groundwater seepage has a great influence on the extent of soil failure in front of the tunnel face of the shield tunnel. When groundwater seepage is considered, the extent of soil failure in front of the excavation face is significantly increased. If the shield tunnel is excavated in groundwater-rich strata, the influence of groundwater seepage on the stability of the tunnel face of the shield tunnel cannot be ignored.

Acknowledgments

This study was supported by the National Natural Science Foundation of China (Grants No. 51878074 and 51908067), Natural Science Foundation of Hunan Province, China (Grant No. 2021JJ30714) and Innovation Driven Project of Central South University (No. 2019CX011). Their financial supports are greatly appreciated.

References

Chen, W.F. (1975), *Limit Analysis and Soil Plasticity*, Elsevier Science, Amsterdam, The Netherlands.

Chen, R.P., Yin, X.S., Tang, L.J. and Chen, Y.M. (2018), "Centrifugal model tests on face failure of earth pressure balance shield induced by steady state seepage in saturated sandy silt ground", *Tunn. Undergr. Sp. Tech.*, **81**, 315-325. https://doi.org/10.1016/j.tust.2018.06.031.

Huang, F., Ou, R.C., Li, Z.L., Yang, X.L. and Ling, T.H. (2018), "Limit analysis for the face stability of a shallow-shield tunnel based on a variational approach to the blow-out failure mode", *Int. J. Geomech.*, **18**(6), 04018038. https://doi.org/10.1061/(ASCE)GM.1943-5622.0001150.

Huang, F., Zhang, M., Wang, F., Ling, T.H. and Yang, X.L. (2020), "The failure mechanism of surrounding rock around an existing shield tunnel induced by an adjacent excavation", *Comput. Geotech.*,**117**, 103236. https://doi.org/10.1016/j.compgeo.2019.103236.

Ibrahim, E., Soubra, A.H., Mollon, G., Raphael, W., Dias, D. and Reda, A. (2015), "Three-dimensional face stability analysis of pressurized tunnels driven in a multilayered purely frictional medium", *Tun. Undergr. Sp. Tech.*, **49**, 18-34. https://doi.org/10.1016/j.tust.2015.04.001.

Leca, E. and Dormieux, L. (1990), "Upper and lower bound solutions forthe face stability of shallow circular tunnels in frictional material", *Geotechnique*, **40**(4), 581-606. https://doi.org/10.1680/geot.1990.40.4.581.

Li, T.Z. and Yang, X.L. (2019), "Three-dimensional face stability of shallow-buried tunnels with tensile strength cut-off", *Comput. Geotech.*, **110**, 82-93. https://doi.org/10.1016/j.compgeo.2019.02.014.

Li, Z.W., Yang, X.L. and Li, T.Z. (2019), "Face stability analysis of tunnels under steady unsaturated seepage conditions", *Tunn. Undergr. Sp. Tech.*, **93**, 103095. https://doi.org/10.1016/j.tust.2019.103095.

Lv, X.L., Zhou, Y.C., Huang, M.S. and Zeng, S. (2018), "Experimental study of the face stability of shield tunnel in sands under seepage condition", *Tunn. Undergr. Sp. Tech.*, **74**, 195-205. https://doi.org/10.1016/j.tust.2018.01.015.

Mollon, G., Dias, D. and Soubra, A.H. (2009), "Probabilistic Analysis and Design of Circular Tunnels against Face Stability", *Int. J. Geomech.*, **9**(6), 237-249. https://doi.org/10.1061/(asce)1532-3641(2009)9:6(237).

Mollon, G., Dias, D. and Soubra, A.H. (2011), "Rotational failure mechanisms for the face stability analysis of tunnels driven by a pressurized shield", *Int. J. Numer. Anal. Met. Geomech.*, **35**(12), 1363-1388. https://doi.org/10.1002/nag.962.

Mollon, G., Dias, D. and Soubra, A.H. (2013), "Continuous velocity fields for collapse and blowout of a pressurized tunnel face in purely cohesive soil", *Int. J. Numer. Anal. Met. Geomech.*, **37**(13), 2061-2083. https://doi.org/10.1002/nag.2121.

Pan, Q.J. and Dias, D. (2016), "The effect of pore water pressure on tunnel face stability", *Int. J. Numer. Anal. Met. Geomech.*, **40**(15), 2123-2136. https://doi.org/10.1002/nag.2528.

Pan, Q.J. and Dias, D. (2018), "Three dimensional face stability of a tunnel in weak rock masses subjected to seepage forces", *Tunn. Undergr. Sp. Tech.*, **71**, 555-566. https://doi.org/10.1016/j.tust.2017.11.003.

Perazzelli, P., Leone, T. and Anagnostou, G. (2014), "Tunnel face stability under seepage flow conditions", *Tunn. Undergr. Sp. Tech.*, **43**, 459-469. https://doi.org/10.1016/j.tust.2014.03.001.

Sahoo, J.P. and Kumar, B. (2019), "Support pressure for stability of circular tunnels driven in granular soil under water table", *Comput. Geotech.*, **109**, 58-68. https://doi.org/10.1016/j.compgeo.2019.01.005.

Senent, S., Mollon, G. and Jimenez, R. (2013), "Tunnel face stability in heavily fractured rock masses that follow the Hoek-Brown failure criterion", *Int. J. Rock Mech. Min. Sci.*, **60**, 440-451. https://doi.org/10.1016/j.ijrmms.2013.01.004.

Zhang, B., Ma, Z.Y., Wang, X., Zhang, J.S. and Peng W.Q. (2020), "Reliability analysis of anti-seismic stability of 3D pressurized tunnel faces by response surfaces method", *Geomech. Eng.*, **20**(1), 43-54. https://doi.org/10.12989/gae.2020.20.1.043.

Zhang, J.H., Wang, W.J., Zhang, D.B., Zhang, B. and Meng, F. (2018), "Safe range of retaining pressure for three-dimensional face of pressurized tunnels based on limit analysis and reliability method", *KSCE J. Civ. Eng.*, **22**(11), 2625-2656. https://doi.org/10.1007/s12205-017-0619-5.

CC